



## OPEN ACCESS

## EDITED BY

Fei Shen,  
Beijing Academy of Agricultural and Forestry  
Sciences, China

## REVIEWED BY

Sen Yang,  
Henan Agricultural University, China  
Pritam Kalia,  
Indian Agricultural Research Institute (ICAR),  
India  
Zhenyu Huang,  
Chinese Academy of Agricultural Sciences,  
China

## \*CORRESPONDENCE

Xinsheng Wu  
✉ wxs@nbweimeng.com  
Nanqiao Liao  
✉ lnqiao@zju.edu.cn

RECEIVED 03 July 2024

ACCEPTED 13 August 2024

PUBLISHED 03 September 2024

## CITATION

Liu J, Fang X, Yu F, Zhang C, Fan P, Wang N,  
Shao Q, Gan N, Lv X, Ouyang B, Zhang M,  
Wu X and Liao N (2024) Genetic mapping and  
molecular marker development for white  
flesh color in tomato.  
*Front. Plant Sci.* 15:1459013.  
doi: 10.3389/fpls.2024.1459013

## COPYRIGHT

© 2024 Liu, Fang, Yu, Zhang, Fan, Wang, Shao,  
Gan, Lv, Ouyang, Zhang, Wu and Liao. This is  
an open-access article distributed under the  
terms of the [Creative Commons Attribution  
License \(CC BY\)](https://creativecommons.org/licenses/by/4.0/). The use, distribution or  
reproduction in other forums is permitted,  
provided the original author(s) and the  
copyright owner(s) are credited and that the  
original publication in this journal is cited, in  
accordance with accepted academic  
practice. No use, distribution or reproduction  
is permitted which does not comply with  
these terms.

# Genetic mapping and molecular marker development for white flesh color in tomato

Jie Liu<sup>1,2</sup>, Xiaoxue Fang<sup>1,2</sup>, Fangjie Yu<sup>1,2</sup>, Chengfeng Zhang<sup>1,2</sup>,  
Pengfei Fan<sup>1,2</sup>, Ningdong Wang<sup>1,2</sup>, Qiao Shao<sup>1,2</sup>, Ning Gan<sup>1,2</sup>,  
Xiaolong Lv<sup>3</sup>, Bo Ouyang<sup>4</sup>, Mingfang Zhang<sup>3</sup>,  
Xinsheng Wu<sup>1,2\*</sup> and Nanqiao Liao<sup>1,2\*</sup>

<sup>1</sup>Department of Molecular Assistant Breeding, Weimeng Seed Co. Ltd., Ningbo, China, <sup>2</sup>Key Laboratory of digital seed industry of watermelon, melon & cabbage, Ministry of Agriculture and Rural Areas, Ningbo, China, <sup>3</sup>Laboratory of Germplasm Innovation and Molecular Breeding, College of Agriculture and Biotechnology, Zhejiang University, Hangzhou, China, <sup>4</sup>Department of Vegetable Science, College of Horticultural and Forest Sciences, Huazhong Agricultural University, Wuhan, China

**Introduction:** Fruit color significantly influences the quality of horticultural crops, which affects phytochemical diversity and consumer preferences. Despite its importance, the genetic basis of the white-colored fruit in tomatoes remains poorly understood.

**Methods:** In this study, we demonstrate that white-fleshed tomato varieties accumulate fewer carotenoids than yellow-fleshed varieties. We developed various segregating populations by hybridizing red, yellow, and white fruit tomato cultivars.

**Results:** Genetic analysis revealed that the white fruit color trait is controlled by a single gene that dominates both red and yellow fruits. Bulk segregant RNA sequencing provided a preliminary map of a 3.17 Mb region on chromosome 3 associated with the white color trait. Based on kompetitive allele-specific PCR (KASP) markers, we narrowed the candidate gene region to 819 kb. Within this region, we identified a 4906-bp sequence absence variation near Phytoene Synthase 1 (SIPSY1) specific to white-colored tomatoes. Genotyping of the progeny and natural populations using a single nucleotide polymorphism adjacent to this absence of variation confirmed its key role in white fruit formation.

**Discussion:** Collectively, our findings provide insights into white fruit trait formation in tomatoes, enabling tomato breeders to precisely introduce white fruit traits for commercial exploitation.

## KEYWORDS

tomato, white flesh, gene mapping, molecular breeding, fruit color

## 1 Introduction

Tomatoes (*Solanum lycopersicum* L.) are among the most important vegetables globally. Annual production of fresh tomatoes is expected to reach approximately 254 million tons by 2022 (<https://www.fao.org/>). Tomatoes are nutritionally well balanced and rich in vitamins and functional pigments, and are important in global food security and nutrition (Chen et al., 2023). The attractiveness of fresh color is a key breeding goal that greatly affects consumer preferences and is determined by pigments in the peel and pericarp (Lin et al., 2014). Plants produce these pigments in flowers and fruits primarily to attract pollinators and seed dispersers (Ballester et al., 2010; Yang et al., 2023). Pigments contribute to both the aesthetic appeal and nutritional benefits of fruits and vegetables favored by consumers. The main pigments in tomatoes include chlorophylls, carotenoids, and flavonoids, which contribute to the red, orange, yellow, green, light green, and white flesh (Li and Yuan, 2013; Kabelka et al., 2004).

Fruit color has been studied for decades as an attractive attribute of horticultural crops. Major genes or quantitative trait loci (QTLs) that influence flesh color have been identified in crops, such as watermelon, melon, cucumber, and peppers. For instance, The *CILCYB* gene encoding lycopene beta-cyclase, which is responsible for the red flesh color in watermelon, has been mapped to chromosome 4 (Liu et al., 2014). The abundance of the protein is inversely correlated with lycopene accumulation (Zhang et al., 2020). Similarly, the golden flesh trait in watermelons is determined by *CIPSY1* (*Phytoene synthase 1*) on chromosome 4 (Liu et al., 2021), whereas scarlet red flesh color ( $Y^{scr}$ ) involves glycine-rich cell wall proteins encoded by candidate genes on chromosome 6 (Li et al., 2020). The plastid lipid-associated protein Cla97C10G185970 likely influences the pale green flesh color in watermelons (Pei et al., 2021). In melon, the *CmOr* gene regulates  $\beta$ -carotene accumulation (Tzuri et al., 2015). The *CmPPR1* gene for white flesh color has been mapped to chromosome 8 (Galpaz et al., 2018). In cucumber, the *ORE* gene on chromosome 3DS is pivotal for  $\beta$ -carotene accumulation (Bo et al., 2011), whereas a single recessive gene (*yf*) on chromosome 7 controls the light yellow flesh color (Lu et al., 2015). In chili pepper, QTLs pc8.1 and pc10.1 influence chlorophyll levels in green-ripe fruits (Brand et al., 2011, 2014), with *CaGLK2* being identified as a candidate gene for pc10.1, which affects chloroplast development, similar to *SlGLK2* from tomato (Brand et al., 2014).

Several major genes associated with flesh color have been identified in tomatoes. The findings have clarified the structural and regulatory pathways that influence mature fruit color. *PSY1* encodes phytoene synthase, a key enzyme in carotenoid biosynthesis that catalyzes the condensation of two geranylgeranyl diphosphate molecules to form 15-cis-phytoene, which is the initial step in carotenoid production (Zhou et al., 2022). Mutants in *PSY1*, such as *r* (yellow flesh) and *r<sup>v</sup>*, result in mature fruits with pale yellow flesh and yellow skin (Fray and Grierson, 1993). Mutation of the carotenoid isomerase gene (*CRTISO*) leads to a significant decrease in carotenoid components downstream of tetra-cis-lycopene, ultimately producing an orange fruit phenotype (Isaacson et al., 2002). *SlMYB12* encodes a crucial transcription factor that regulates naringin chalcone biosynthesis in tomatoes. Deletion of this gene results in a colorless

epidermis due to flavonoid deficiency, although the flesh remains red, giving the fruit a pink appearance (Ballester et al., 2010; Zhu et al., 2018). Chlorophyll influences tomato coloration. Mutations in *STAY-GREEN* (*SGR*) inhibit chlorophyll degradation during ripening (Pereira-Castro and Moreira, 2021), leading to the accumulation of lycopene and brown-colored fruits (Barry et al., 2008). A CRISPR/Cas9-mediated multiplex gene editing system was used to successfully generate differently colored fruits of tomato lines from red-fruited materials by editing three fruit-color-related genes (*PSY1*, *MYB12*, and *SGR1*) (Yang et al., 2023).

Diverse fruit color patterns are favored by both breeders and consumers. White flesh tomato varieties, which harbor natural mutations commonly used in tomato breeding, are particularly attractive because of their distinct fruit color. Here, a series of genetic mappings and molecular analyses of white flesh traits in tomatoes were performed. The white flesh trait was dominant over both red and yellow flesh traits. Using fine mapping approach, we narrowed down the white flesh gene to an 819-kb region and identified a 4906 bp sequence deletion near the *PSY1* gene. This is likely the causal variant for white flesh. Our findings provide valuable genetic resources and insight into the structural variations associated with tomato coloration.

## 2 Materials and methods

### 2.1 Plant materials and phenotyping

A white commercial hybrid variety, BaiFei (BF), was obtained from a seed market and used as a genetic resource for white fruit traits. The hybrid seeds ZheYingFen (ZYF) and JinGuan16 were used as genetic resources for red and yellow fruit traits, respectively. Four parent hybrids ( $F_1$ ) were generated by crossing BF with ZYF or JG16.  $F_2$  populations were produced by self-crossing the four parent hybrids, whereas  $F_3$  populations resulted from self-crossing  $F_2$  materials. Most experiments were performed under greenhouse conditions at JiangShan Farm, Weimeng Seed Co., Ltd. (Ningbo, Zhejiang Province, China). Tomato flesh color was observed after exocarp peeling. The pedigree diagram for the hybrid materials used in this study is provided in Supplementary Figure 1.

### 2.2 Detection of carotenoids

Carotenoid extraction and determination by high-performance liquid chromatography (HPLC) was performed referring to the previously described protocol (Lu et al., 2018). The methods of carotenoid detection on Carotenoid content was analyzed using Metware (<http://www.metware.cn/>) using the triple quadrupole-linear ion trap (QTRAP<sup>®</sup>) 6500+ liquid chromatography-tandem mass spectrometry (LC-MS/MS) platform (AB Sciex, Toronto, ON, Canada). Approximately 50 mg of freeze-dried ground powder was sampled and extracted with a 0.5 mL mixed solution of n-hexane, acetone, and ethanol (1:1:1, v/v/v). The sample was vortexed for 20 min at room temperature, and supernatants were collected after centrifugation at 12,000 r/min for 5 min at 4°C. The residue was subjected to a second extraction using the same procedure, dried, and

reconstituted in 100  $\mu$ L of dichloromethane. The resulting solution was filtered through a 0.22  $\mu$ m membrane filter for LC-MS/MS analysis. Sample extracts were analyzed using an ultraperformance LC-atmospheric-pressure chemical ionization-tandem mass spectrometry (UPLC-APCI-MS/MS) system, with UPLC performed using an ExionLC<sup>TM</sup> AD device and MS performed using a model 6500 Triple Quadrupole instrument (Applied Biosystems, Waltham, MA, USA). The experimental parameters were set as follows. For the LC system, a YMC C30 column (3  $\mu$ m, 100 mm  $\times$  2.0 mm) was used, with a solvent system of methanol and acetonitrile (1:3, v/v) containing 0.01% butylated hydroxytoluene (BHT) and 0.1% formic acid (A), and methyl tert-butyl ether with 0.01% BHT (B). The gradient program was 0% B from 0 to 3 min, increased to 70% B from 3 to 5 min, further increased to 95% B from 5 to 9 min, and returned to 0% B from 10 to 11 min. The flow rate was maintained at 0.8 mL/min, column temperature at 28°C, and injection volume at 2  $\mu$ L. Detection was performed using both linear ion trap and triple quadrupole scans on the aforementioned QTRAP<sup>®</sup> 6500+ LC-MS/MS System equipped with an APCI Heated Nebulizer, operating in positive ion mode and controlled by Analyst 1.6.3 software (AB Sciex). The APCI source operated with the ion source set to APCI+, source temperature of 350°C, and curtain gas (CUR) set to 25.0 psi. Carotenoids were analyzed using scheduled multiple reaction monitoring (MRM), and data acquisition was conducted using Analyst 1.6.3 software (AB Sciex). Quantification of all metabolites was performed using MultiQuant 3.0.3 software (AB Sciex). MS parameters, including declustering potential (DP) and collision energy (CE) for individual MRM transitions, were optimized through further adjustments of DP and CE. A specific set of MRM transitions was monitored for each period based on the elution of metabolites.

## 2.3 Bulk segregant RNA sequencing analysis

RNA was extracted from mature fruit flesh using the RNeasy Pure Extraction Kit (Qiagen Biotech, Beijing, China) according to the manufacturer's recommendations. Two pools were created, the W1-pool and Y-pool, representing white and yellow fruit flesh samples, respectively, by mixing 20 individuals each from the BF\*JG16 populations. Similarly, the W2-pool and R-pool representing the white and red fruit flesh samples, respectively, were constructed from the BF\*ZYF populations. RNA sequencing generated 150 bp paired-end reads with an insert size of approximately 350 bp. Sequencing libraries were prepared using the Truseq Nano DNA HT Sample Preparation Kit (Illumina, San Diego, CA, USA) and sequenced on the Illumina HiSeq4000 platform. The quality of sequencing data was assessed using FastQC (<https://github.com/s-andrews/FastQC/>), followed by filtering of low-quality reads. The Mutation Mapping Analysis Pipeline for Pooled RNA-seq (MMAPPR) pipeline was used for BSR (Hill et al., 2013).

## 2.4 Fine mapping

Genotyping was performed using competitive allele-specific PCR assays based on kompetitive allele-specific PCR (KASP<sup>TM</sup>) technology

(LGC Genomics, Teddington, Middlesex, UK) at LGC Genomics. Single nucleotide polymorphisms (SNPs) detected in the candidate region were selected to design KASP markers (Supplementary Table 5). The KASP assay mix was blended with 100 ng/ $\mu$ L FAM, 100 ng/ $\mu$ L HEX, 100 ng/ $\mu$ L R, and distilled deionized water, with a volume ratio of 12:12:30:46. The KASP reaction was performed in a reaction volume of 5.07  $\mu$ L, with 2.5  $\mu$ L DNA, 2.5  $\mu$ L KASP master mix and 0.07  $\mu$ L KASP assay mix. The KASP protocol comprised the stage 1 pre-read stage of 30°C for 1 min; stage 2 hold stage of 94°C for 15 min; stage 3 PCR stage (touchdown) for 94°C for 20 s then 61°C for 1 min (decrease of 0.6°C), recycling nine times (a total of 10 cycles), achieving a final annealing temperature of 55°C; stage 4 PCR stage of 94°C for 20 s, 55°C for 1 min, and recycling 26 times; and stage 5 post-read stage of 30°C for 1 min. After amplification, an LGC Omega F reader was used to detect the fluorescence signal and validate the classification. Further cycles were conducted if the genotyping was insufficient, and the results were validated.

## 2.5 Cloning and RT-qPCR analysis of candidate gene

F<sub>4</sub> individuals (BF\*ZYF-8-2-1 and BF\*ZYF-11-1-8) exhibiting pure white or yellow phenotypes were used to amplify the candidate gene and conduct gene expression analysis. PCR amplification was performed using KOD ONE PCR Master Mix (Toyobo, Osaka, Japan). Gene expression levels at the breaker and mature stages were examined by RT-qPCR. Total RNA was isolated using the RNeasy Pure Extraction Kit (Qiagen), assessed for quality by 1% agarose gel electrophoresis, and converted to cDNA using HiScript II Q RT SuperMix for qPCR (+gDNA wiper) (Cat no. R223, Vazyme, Shanghai, China). PCR was performed using the ChamQ Universal SYBR qPCR Master Mix (Cat No. Q711-02, Toyobo), on a CFX96 Touch Real-Time PCR Detection System (Bio-Rad, Hercules, CA, USA). The tomato actin gene was used as an internal control and all analyses were performed with three biological and technical replicates. All primers used for RT-qPCR are listed in Supplementary Table 6.

## 3 Results

### 3.1 Difference in metabolites between white and yellow fruit flesh in tomatoes

Carotenoids are known for their antioxidant, anticancer, and vision-supporting properties and typically impart orange, red, and yellow colors to flowers and fruits (Liu et al., 2015). To investigate the phenotypic differences between white- and yellow-flesh tomato fruits, two F<sub>4</sub> populations, BF\*ZYF-8-2-1 (Yellowish white flesh, number 155D, Horticulture Royal Society Chart) and BF\*ZYF-11-1-8 (Vivid yellow flesh, number 9B, Horticulture Royal Society Chart), were selected to assess carotenoid variation (Figures 1A, B). Carotenoids can be categorized into two main groups: xanthophylls and carotenes (Liu et al., 2015). In yellow fruits,  $\beta$ -carotene was identified as the predominant carotene, which was significantly higher compared to white flesh fruits (Figure 1C). Lycopene,

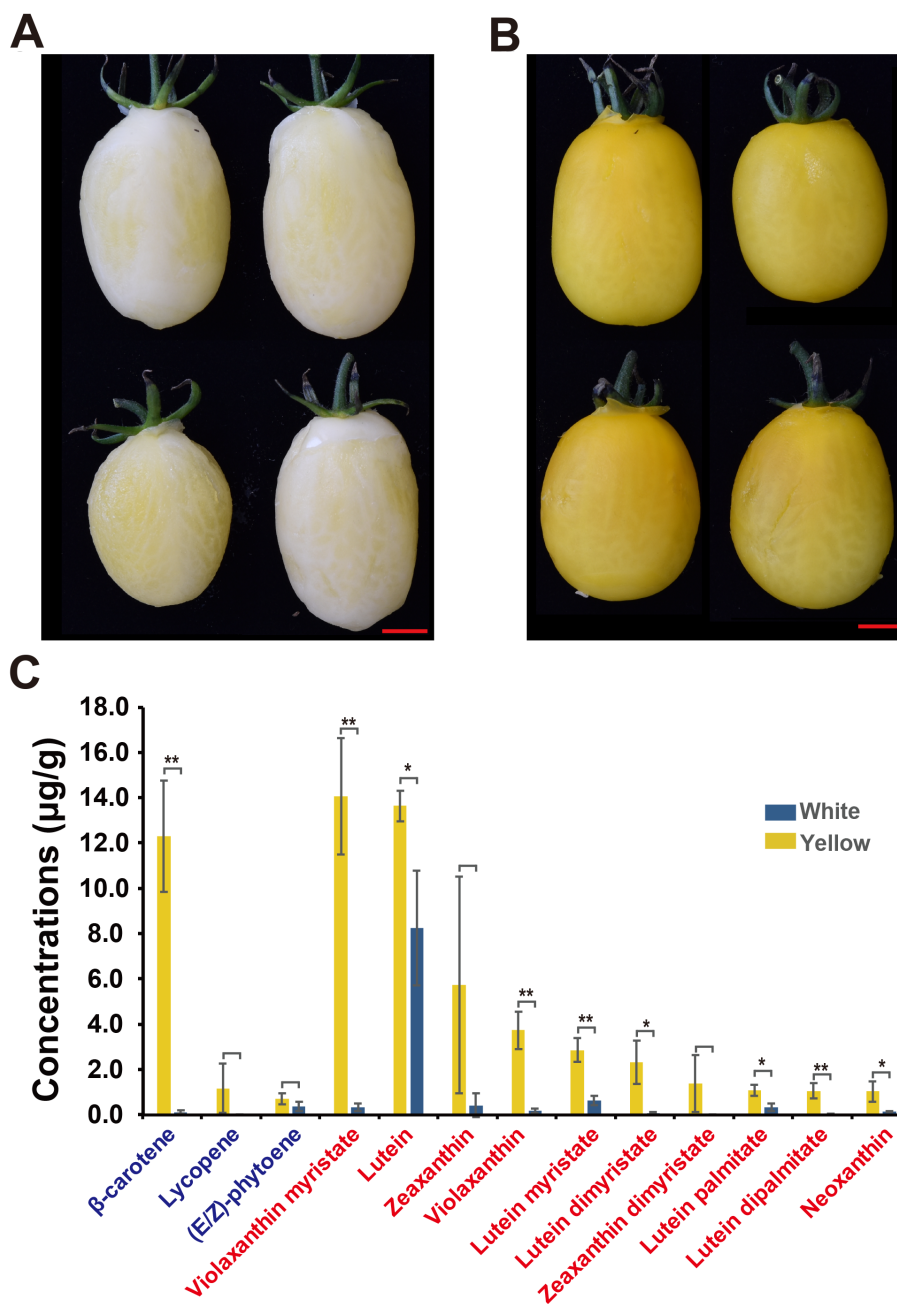


FIGURE 1

Tomato fruit color phenotypes and carotenoid concentrations in white and yellow flesh fruits. (A, B) Illustrations of (A) white (BF\*ZYF-8-2-1) and (B) yellow (BF\*ZYF-11-1-8) flesh fruit colors. (C) Carotenoid concentrations in white and yellow flesh fruits. Carotenes are marked in blue, and xanthophylls are marked in red. Student's *t*-test, \*\* $P < 0.01$ , \* $P < 0.05$ .

typically abundant in red tomato fruits, was present in trace amounts in yellow fruits and was undetectable in white fruits. Small amounts of (E/Z)-phytoene were detected in both yellow and white fruits. Regarding xanthophylls, yellow fruits showed a trend of higher accumulation than white fruits (Figure 1; Supplementary Table 1), notably violaxanthin myristate, which exhibited significant differences between the groups. Overall, white fruits accumulated fewer carotenoids than yellow fruits.

### 3.2 Inheritance pattern of white fruit color in tomatoes

To explore the inheritance pattern of white fruit color in tomatoes, two sets of  $F_3$  populations derived from the four parent hybrids were analyzed. For white and yellow traits, four  $F_3$  populations initially displayed white flesh phenotypes, with subsequent observations revealing 50 yellow and 143 white fruit

offspring (Table 1). The ratio observed fits a Mendelian ratio ( $\chi^2 = 0.694$ ,  $P = 0.45$ ), indicating that white fruit color is dominant to yellow in this population. Similarly, for the white and red flesh traits, eight out of 16 populations, starting with a white phenotype, exhibited pure white fruit phenotypes. The remaining populations comprised 89 red and 217 white individuals (Table 1), fitting a Mendelian ratio ( $\chi^2 = 2.7233$ ,  $P = 0.099$ ), suggesting the dominance of white fruit color over red in this population.

### 3.3 Genetic mapping of the candidate locus for white fruit color

To identify candidate loci associated with white fruit color in tomatoes, BSR analysis was performed. Equal quantities of RNA from the flesh of 20 white and 20 yellow tomatoes from the BF\*HG16 population were pooled to generate White1\_pool and Yellow\_pool, respectively. Similarly, RNA from 20 white and 20 red tomatoes from the BF\*ZYP population was pooled to create the White2\_pool and Red\_pool. Sequencing of these four pools generated 25.05 Gb of raw data, with Q20 > 98.11%, Q30 > 94.45%, and guanine-cytosine ratios ranging from 42.76% to 43.13% (Supplementary Table 2). A BSR analysis pipeline was employed to identify candidate regions. For the White1\_pool and

yellow pool, three significant peaks above the threshold were detected (Figure 2A; Supplementary Table 3). Similarly, the White2\_pool and red pool showed four significant peaks above the threshold (Figure 2B). Chromosome 3 showed the most significant peak in both analyses, with an overlapping region (SL4.0ch03:3665098-6832118) identified as a candidate region.

### 3.4 4906-bp sequence absence near *PSY1* confers white fruit trait

To validate this candidate region, we mapped RNA-seq reads to the reference genome and identified variations that served as a source for SNP marker selection. Two markers, Chr03:4312942 and Chr03:4485072, showed genotype segregation and were used to genotype F<sub>3</sub> populations. Strong correlations between genotype and phenotype were observed in the XT-5 population from the BF\*HG16 offspring and in XT-54, XT-56, and XT-56 from the BF\*ZYP offspring (Supplementary Table 4). We then selected offspring from the heterozygous lines in the XT-5 population for further fine mapping. Four markers (Chr03:4312942, Chr03:4485072, Chr03:4580102, and Chr03:4586240; details in Supplementary Table 5) exhibited genotype segregation in XT-3 populations and were used to screen recombinants. After screening

TABLE 1 Phenotypes of segregation populations.

Population Code	Genealogical information	Pre-generation phenotype	Phenotype		
			Yellow	Red	White
XT-3	BF*HG16-1-1	white	12	/	36
XT-4	BF*HG16-1-4	white	11	/	38
XT-5	BF*HG16-3-7	white	16	/	31
XT-6	BF*HG16-6-2	white	14	/	34
XT-40	BF*ZYP-8-1	white	/	0	40
XT-41	BF*ZYP-8-2	white	/	0	40
XT-42	BF*ZYP-8-3	white	/	0	40
XT-43	BF*ZYP-11-1	white	/	13	22
XT-44	BF*ZYP-11-2	white	/	11	27
XT-45	BF*ZYP-11-3	white	/	0	40
XT-46	BF*ZYP-12-1	white	/	0	40
XT-50	BF*ZYP-20-1	white	/	14	25
XT-51	BF*ZYP-20-2	white	/	0	40
XT-52	BF*ZYP-22-1	white	/	13	27
XT-53	BF*ZYP-22-2	white	/	9	29
XT-54	BF*ZYP-24-1	white	/	12	27
XT-55	BF*ZYP-24-2	white	/	0	40
XT-56	BF*ZYP-26-1	white	/	9	29
XT-58	BF*ZYP-26-3	white	/	8	31
XT-59	BF*ZYP-26-4	white	/	0	40

\* means hybridization, detail information is provided in Supplementary Figure 1.



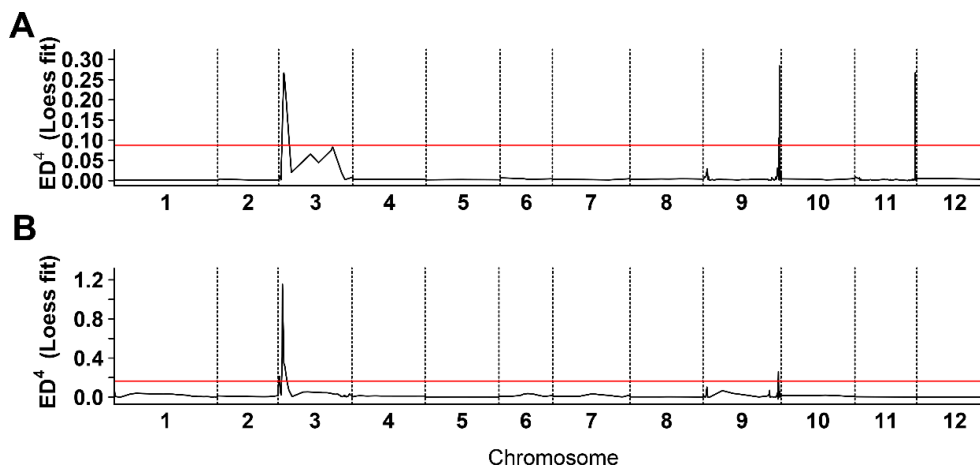


FIGURE 2

Bulk segregant RNA-seq analysis of white flesh in tomato. (A) Distribution of Euclidean distance (ED) association values across chromosomes in BF\*HG16 population. (B) Distribution of ED association values across chromosomes in BF\*ZYP population. The x-axis denotes chromosome names, the black line represents fitted ED values, and the red line indicates the significance association threshold. Higher ED values indicate stronger single nucleotide polymorphisms locus associations.

approximately 1500  $F_4$  individuals, we identified 37 recombinants with pure white or heterozygous genotypes, refining the candidate genes to an 819 kb region (SL4.0ch03:3665098–4485072) based on recombinant genotypes and phenotypes (Figure 3).

To identify the causal gene for white flesh formation in tomatoes, we resequenced  $F_4$  individuals (BF\*ZYP-8-2-1 and BF\*ZYP-11-1-8) with pure white or yellow phenotypes. A 4906-bp sequence was absent near *PSY1* in whites. The deletion results in the absence of the 3' untranslated region (UTR) of *PSY1* and the initiation codon of *SolyC03g031870* (Figure 4A), which encodes an Acyl-CoA synthetase that is crucial for pollen development, male fertility, and thermotolerance (Hu et al., 2020; Xie et al., 2024). Gel markers designed for genotyping confirmed that the deletion was exclusively detected in white flesh germplasm (Figure 4B; Supplementary Table 6), and a nearby SNP marker (Chr3:4285980; Figure 4C) further validated this finding. Gene expression analysis revealed significantly higher *PSY1* expression in yellow flesh than in white fruit (Figure 4D), whereas *SolyC03g031870* expression was undetectable in both varieties. Therefore, we conclude that this deletion likely affects the expression of *PSY1*, leading to the formation of white flesh.

To explore whether the variability in flesh color across natural populations can be explained by this gene, we examined the resequencing results from accessions of various colors. Remarkably, causal deletions were only found in white fruit varieties based on read coverage in this region (Supplementary Table 7), which was corroborated by structural variation and nearby SNP markers (Figure 4D). These findings highlight that the deletion is the causal variant in white flesh formation. In addition, we developed a KASP marker that was close to the deletion. The genotyping results confirmed that the GG genotype was exclusive to white varieties (Figure 4D), suggesting its utility in further molecular breeding.

## 4 Discussion

Carotenoids are essential pigments synthesized by plants. These pigments enrich the vibrant spectrum of color found in fruits (Khoo et al., 2011). The presence and distribution of carotenoids within fruit tissues are fundamental determinants of fruit coloration and significantly influence consumer preference.  $\beta$ -carotene, lycopene, and lutein are among the key carotenoids responsible for infusing fruits with their characteristic yellow, orange, and red hues, respectively (Saini et al., 2015). Synthesized primarily within chloroplasts during fruit ripening via a sequence of enzymatic reactions, carotenoid biosynthesis is orchestrated by pivotal genes that include *PSY* (Yang et al., 2023). The tomato genome possesses three *PSY* genes, *PSY1*, *PSY2*, and *PSY3*, each exhibiting distinct tissue-specific expression patterns, predominantly in the fruit, petals, and roots (Fraser et al., 2001, 2007). Throughout tomato ripening, the expression of *PSY1* closely correlates with the accumulation of carotenoids, which in turn influences the final coloration of the fruit (Ray et al., 1992; Cao et al., 2023). Reductions in total carotenoid content are observed in fruits with yellow flesh when *PSY1* is subjected to antisense silencing, gene editing or knock-out mutations (Ray et al., 1992; Cao et al., 2023; Yang et al., 2023). Conversely, overexpression of this gene leads to increased levels of  $\beta$ -carotene (Fraser et al., 2007).

Similar findings regarding the correlation between upregulated *PSY* gene expression and heightened carotenoid accumulation have been documented across various fruits and thus resulted in color changes, including pepper (Rodriguez-Urbe et al., 2012), citrus (Peng et al., 2013), loquat (Xiumin et al., 2014), watermelon (Pin et al., 2015), and raspberry (Mizuno et al., 2017). For example, *CIPSY1* plays a dominant role in carotenoid biosynthesis during the ripening of watermelon fruit, with its expression significantly lower in the white-fleshed variety compared to the pigmented fruits in

Code	Chr03:4285980	Chr03:4312942	Chr03:4485072	Chr03:4580102	Chr03:4586240	Chr03:5004573	Phenotype
F4-128	1	1	2	2	2	2	White
F4-244	1	1	2	2	2	2	White
F4-290	1	1	2	2	2	2	White
F4-389	0	0	2	2	2	1	White
F4-652	1	1	1	1	2	2	White
F4-771	1	1	1	2	2	2	White
F4-781	1	1	1	2	2	2	White
F4-795	1	1	2	2	2	2	White
F4-826	1	1	2	2	2	2	White
F4-914	1	1	2	2	2	1	White
F4-1083	1	1	1	2	2	2	White
F4-1101	1	1	2	2	2	2	White
F4-1169	1	1	2	2	2	2	White
F4-1184	1	1	2	2	2	2	White
F4-1260	1	1	2	2	2	2	White
F4-1268	1	1	1	2	2	2	White
F4-1311	1	1	2	2	2	2	White
F4-1412	1	1	2	2	2	2	White
F4-132	2	2	1	1	1	1	Yellow
F4-192	2	2	1	1	1	1	Yellow
F4-195	2	2	1	1	1	1	Yellow
F4-251	2	2	1	1	1	1	Yellow
F4-274	2	2	1	1	1	1	Yellow
F4-278	2	2	0	0	0	0	Yellow
F4-357	2	2	1	1	1	1	Yellow
F4-401	2	2	1	1	1	1	Yellow
F4-453	2	2	1	1	1	1	Yellow
F4-611	2	2	1	1	1	1	Yellow
F4-671	2	2	1	1	1	1	Yellow
F4-863	2	2	1	1	1	1	Yellow
F4-963	2	2	1	1	1	1	Yellow
F4-975	2	2	1	1	1	1	Yellow
F4-1081	2	2	1	1	1	1	Yellow
F4-1215	2	2	2	1	1	1	Yellow
F4-1236	2	2	1	0	0	0	Yellow
F4-1305	2	2	1	1	1	1	Yellow
F4-1393	2	2	2	1	1	1	Yellow

FIGURE 3

Fine mapping and genotyping results of the candidate region. Genotyping result of six KASP markers in typical  $F_4$  recombinant lines. Green indicates homozygous white genotypes, red indicates homozygous yellow genotypes, and yellow indicates heterozygous regions.

watermelon (Fang et al., 2022). Similarly, *ZmPSY1* plays a crucial role in carotenogenesis within the endosperm (Li et al., 2008). Furthermore, the activation of the native *PSY1* promoter has been shown to induce carotenoid biosynthesis in embryogenic rice callus (Sobrinho-Mengual et al., 2024).

Tomatoes have served as a prominent model for studying carotenoid metabolism, revealing a spectrum of phenotypes associated with various *PSY1* variations, such as yellow, tangerine, white, and bicolor phenotypes (Fray and Grierson, 1993; Pereira-Castro and Moreira, 2021; Bulot et al., 2022). A 3789-bp deletion in the *PSY1* promoter has been identified as the causal variation for the bicolor phenotype in tomatoes (Bulot et al., 2022), whereas a duplication and inversion involving *PSY1* and an adjacent gene has been verified as the causal variation in the  $r^y$  phenotype (Bulot et al., 2022). In addition, the insertion of a single long terminal repeat from the Rider transposon in the first exon of *PSY1* resulted in a non-functional protein, which was identified as the determinant of yellow flesh cultivars (Fray and Grierson, 1993). Mutants  $r^{2997}$  and  $r^{3576}$  in the *PSY1* gene

caused yellow flesh phenotypes, whereas the double mutant  $r^{3576}/t^{3406}$  exhibits a typical yellow flesh phenotype, and the double mutant  $r^{2997}/t^{3406}$  shows tangerine phenotypes (Kachanovsky et al., 2012). The 3'-UTR is a critical region, harboring cis-elements that affect an mRNA's processing, localization, translation, and stability, is pivotal in gene regulation and could act as regulatory hubs for the environmental control of gene expression (Pereira-Castro and Moreira, 2021; Emma and Martin, 2024). For instance, a T-DNA insertion in the 3'-UTR of SIFAF1/2c results in a gain-of-function mutation that disrupts the regulatory function of the 3'-UTR, leading to increased expression of SIFAF1/2c in tomato (Zhang et al., 2023). Moreover, research on rice revealed that a stowaway-like MITE (sMITE) embedded in the 3'-UTR of OsGhd2 repress the gene expression and thus affected the grain number, plant height, and heading date (Shen et al., 2017). Here, we identified a 4906-bp sequence absence at the 3' end of the *PSY1* gene in white flesh in tomato, which might be responsible for the white flesh phenotype. The decreased expression of *PSY1* in white fruits

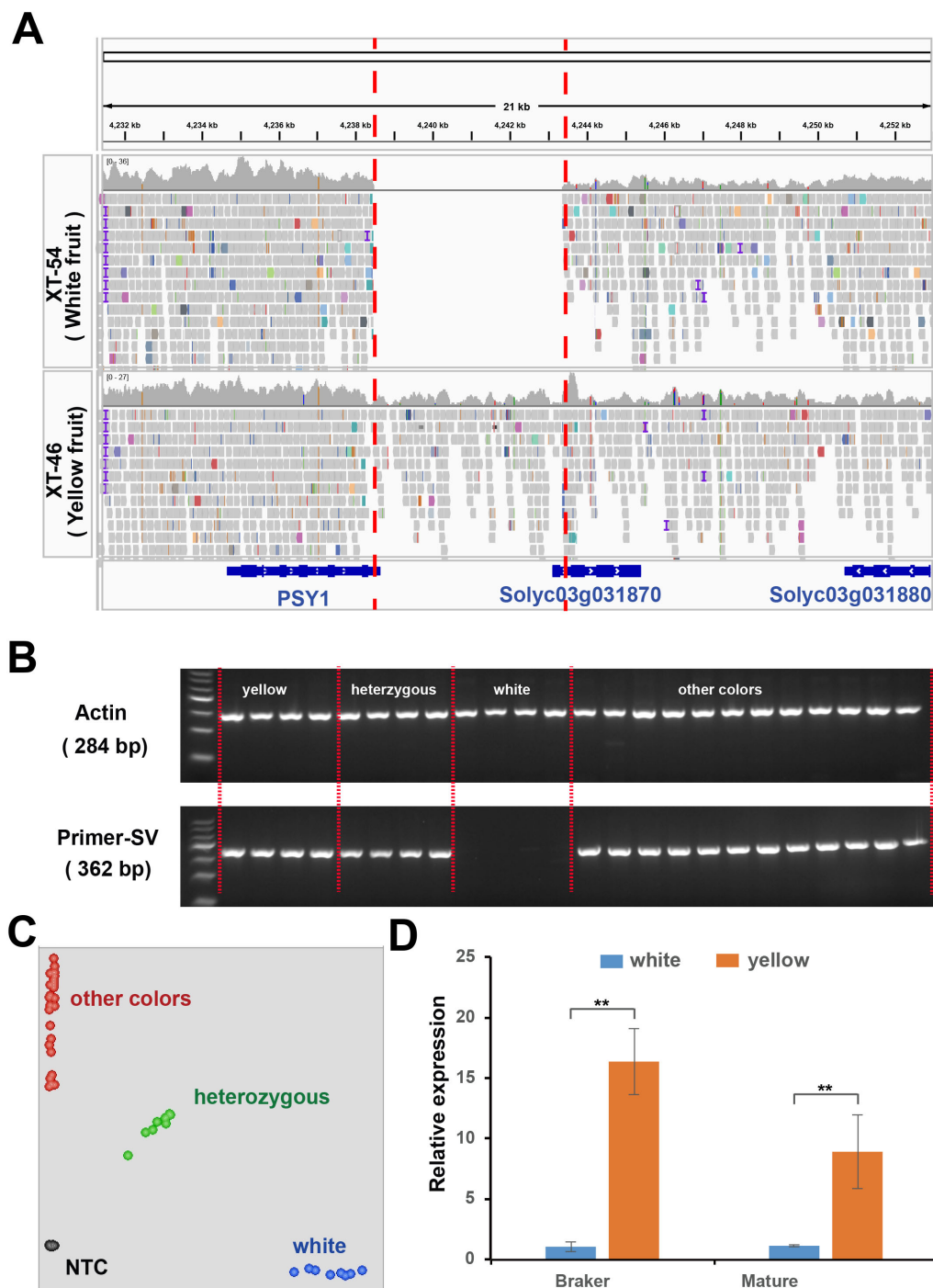


FIGURE 4

Structure variations related to white flesh phenotypes. (A) Re-sequencing results of pure white and pure yellow genotypes in the 21 kb candidate region near *PSY1*. Colored squares indicate the re-sequencing results, with gene structures depicted in blue. (B) PCR analysis of the co-dominant marker InDel-White in the parental lines. (C) KASP analysis of the single nucleotide polymorphism adjacent to the absent fragments. (D) Relative expression of *PSY1* in homozygous white and yellow individuals. Student's t-test, \*\*  $P < 0.01$ .

(Figure 4) provides additional supporting evidence. Thus, it is reasonable to speculate that this deletion may be a causal factor for white flesh formation.

Our study identified a novel variation of *PSY1* underlying the unique white flesh coloration observed in tomatoes. Specifically, structural variation involving a 4906-bp fragment

near *PSY1*, which significantly correlates with the manifestation of white flesh phenotypes, was absent in white flesh tomato germplasm. These findings offer valuable insights into the molecular pathways governing fruit coloration and facilitate advancements in the molecular breeding of white flesh tomato varieties.



## Data availability statement

The datasets presented in this study can be found in online repositories. The names of the repository/repositories and accession number(s) can be found in the article/[Supplementary Material](#).

## Author contributions

JL: Conceptualization, Formal analysis, Methodology, Writing – original draft, Writing – review & editing. XF: Methodology, Validation, Writing – original draft. FY: Methodology, Validation, Writing – original draft. CZ: Methodology, Validation, Writing – original draft. PF: Methodology, Validation, Writing – original draft. NW: Investigation, Writing – original draft. QS: Investigation, Writing – original draft. NG: Investigation, Writing – original draft. XL: Supervision, Writing – original draft, Writing – review & editing. BO: Supervision, Writing – review & editing. MZ: Supervision, Writing – review & editing. XW: Funding acquisition, Project administration, Supervision, Validation, Writing – original draft, Writing – review & editing. NL: Data curation, Investigation, Software, Writing – original draft, Writing – review & editing.

## Funding

The author(s) declare financial support was received for the research, authorship, and/or publication of this article. This

## References

- Ballester, A. R., Molthoff, J., de Vos, R., Hekkert, B. T., Orzaez, D., Fernandez-Moreno, J. P., et al. (2010). Biochemical and molecular analysis of pink tomatoes: deregulated expression of the gene encoding transcription factor SIMYB12 leads to pink tomato fruit color. *Plant Physiol.* 152, 71–84. doi: 10.1104/pp.109.147322
- Barry, C. S., McQuinn, R. P., Chung, M.-Y., Besuden, A., and Giovannoni, J. J. (2008). Amino Acid Substitutions in Homologs of the STAY-GREEN Protein Are Responsible for the green-flesh and chlorophyll retainer Mutations of Tomato and Pepper. *Plant Physiol.* 147, 179–187. doi: 10.1104/pp.108.118430
- Bo, K., Song, H., Shen, J., Qian, C., Staub, J. E., Simon, P. W., et al. (2011). Inheritance and mapping of the ore gene controlling the quantity of  $\beta$ -carotene in cucumber (*Cucumis sativus* L.) endocarp. *Mol. Breed.* 30, 335–344. doi: 10.1007/s11032-011-9624-4
- Brand, A., Borovsky, Y., Hill, T., Rahman K.A., K., Bellalou, A., Van Deynze, A., et al. (2014). CaGLK2 regulates natural variation of chlorophyll content and fruit color in pepper fruit. *Theor. Appl. Genet.* 127, 2139–2148. doi: 10.1007/s00122-014-2367-y
- Brand, A., Borovsky, Y., Meir, S., Rogachev, I., Aharoni, A., and Paran, I. (2011). pc8.1, a major QTL for pigment content in pepper fruit, is associated with variation in plastid compartment size. *Planta.* 235, 579–588. doi: 10.1007/s00425-011-1530-9
- Bulut, B., Isabelle, S., Montoya, R., Nadeau, L. F., Tremblay, J., and Goulet, C. (2022). Structural variations in the phytoene synthase 1 gene affect carotenoid accumulation in tomato fruits and result in bicolor and yellow phenotypes. *bioRxiv*. doi: 10.1101/2022.10.29.514357
- Gao, X., Du, R., Xu, Y., Wu, Y., Ye, K., Ma, J., et al. (2023). Phytoene synthases 1 modulates tomato fruit quality through influencing the metabolic flux between carotenoid and flavonoid pathways. *Hortic. Plant J.* doi: 10.1016/j.hpj.2022.09.015
- Chen, Y., Qiu, S., Zhou, H., Gao, W., Cui, L., Qiu, Z., et al. (2023). Construction of a tomato (*Solanum lycopersicum* L.) introgression line population and mapping of major agronomic quantitative trait loci. *Horticulturae* 9 (7), 823. doi: 10.3390/horticulturae9070823
- Emma, C. H., and Martin, B. (2024). Untranslated yet indispensable—UTRs act as key regulators in the environmental control of gene expression. *J. Exp. Bot.* 75, 4314–4331. doi: 10.1093/jxb/erae073
- Fang, X., Gao, P., Luan, F., and Liu, S. (2022). Identification and characterization roles of phytoene synthase (PSY) genes in watermelon development. *Genes (Basel)*. 13, 1189. doi: 10.3390/genes13071189
- Fraser, P. D., Enfissi, E. M. A., Halket, J. M., Truesdale, M. R., Yu, D. M., Gerrish, C., et al. (2007). Manipulation of phytoene levels in tomato fruit: Effects on isoprenoids, plastids, and intermediary metabolism. *Plant Cell.* 19, 4131–4132. doi: 10.1105/tpc.106.049817
- Fraser, P. D., Römer, S., Kiano, J. W., Shipton, C. A., Mills, P. B., Drake, R., et al. (2001). Elevation of carotenoids in tomato by genetic manipulation. *J. Sci. Food Agric.* 81, 822–827. doi: 10.1002/jsfa.908
- Fray, R. G., and Grierson, D. (1993). Identification and genetic analysis of normal and mutant phytoene synthase genes of tomato by sequencing, complementation and co-suppression. *Plant Mol. Biol.* 22, 589–602. doi: 10.1007/BF00047400
- Galpaz, N., Gonda, I., Shem-Tov, D., Barad, O., Tzuri, G., Lev, S., et al. (2018). Deciphering genetic factors that determine melon fruit-quality traits using RNA-Seq-based high-resolution QTL and eQTL mapping. *Plant J.* 94, 169–191. doi: 10.1111/tj.13838
- Hill, J. T., Demarest, B. L., Bisgrove, B. W., Gorski, B., Su, Y. C., and Yost, H. J. (2013). MMAPP: mutation mapping analysis pipeline for pooled RNA-seq. *Genome Res.* 23, 687–697. doi: 10.1101/gr.146936.112
- Hu, Y., Mesihovic, A., Jimenez-Gomez, J. M., Roth, S., Gebhardt, P., Bublak, D., et al. (2020). Natural variation in HsfA2 pre-mRNA splicing is associated with changes in thermotolerance during tomato domestication. *New Phytol.* 225, 1297–1310. doi: 10.1111/nph.16221
- Isaacson, T., Ronen, G., Zamir, D., and Hirschberg, J. (2002). Cloning of tangerine from tomato reveals a carotenoid isomerase essential for the production of  $\beta$ -carotene and xanthophylls in plants. *Plant Cell.* 14, 333–342. doi: 10.1105/tpc.010303
- Kabelka, E. A., Yang, W., and Francis, D. M. (2004). Improved Tomato Fruit Color within an Inbred Backcross Line Derived from *Lycopersicon esculentum* and *L. hirsutum* Involves the Interaction of Loci. *J. Am. Soc. Hortic. Sci.* 129, 250–257. doi: 10.21273/JASHS.129.2.0250

research was funded by the Major Project of Science and Technology Innovation 2025 of Ningbo City (grant number 2019B10002).

## Conflict of interest

Authors JL, XF, FY, CZ, PF, NW, QS, NG, XW, NL were employed by Weimeng Seed Co. Ltd. The remaining authors declare that the research was conducted in the absence of any commercial or financial relationships that could be construed as a potential conflict of interest.

## Publisher's note

All claims expressed in this article are solely those of the authors and do not necessarily represent those of their affiliated organizations, or those of the publisher, the editors and the reviewers. Any product that may be evaluated in this article, or claim that may be made by its manufacturer, is not guaranteed or endorsed by the publisher.

## Supplementary material

The Supplementary Material for this article can be found online at: <https://www.frontiersin.org/articles/10.3389/fpls.2024.1459013/full#supplementary-material>

- Kachanovsky, D. E., Filler, S., Isaacson, T., and Hirschberg, J. (2012). Epistasis in tomato color mutations involves regulation of phytoene synthase 1 expression by cis-carotenoids. *Proc. Natl. Acad. Sci.* 109, 19021–19026. doi: 10.1073/pnas.1214808109
- Khoo, H.-E., Prasad, K. N., Kong, K.-W., Jiang, Y., and Ismail, A. (2011). Carotenoids and their isomers: color pigments in fruits and vegetables. *Molecules*. 16, 1710–1738. doi: 10.3390/molecules16021710
- Li, N., Shang, J., Wang, J., Zhou, D., Li, N., and Ma, S. (2020). Discovery of the genomic region and candidate genes of the scarlet red flesh color ( $Y^{scr}$ ) locus in watermelon (*Citrullus lanatus* L.). *Front. Plant Sci.* 11. doi: 10.3389/fpls.2020.00116
- Li, F., Vallabhaneni, R., Yu, J., Rocheford, T., and Wurtzel, E. T. (2008). The maize phytoene synthase gene family: overlapping roles for carotenogenesis in endosperm, photomorphogenesis, and thermal stress tolerance. *Plant Physiol.* 147, 1334–1346. doi: 10.1104/pp.108.122119
- Li, L., and Yuan, H. (2013). Chromoplast biogenesis and carotenoid accumulation. *Arch. Biochem. Biophys.* 539, 102–109. doi: 10.1016/j.abb.2013.07.002
- Lin, T., Zhu, G., Zhang, J., Xu, X., Yu, Q., Zheng, Z., et al. (2014). Genomic analyses provide insights into the history of tomato breeding. *Nat. Genet.* 46, 1220–1206. doi: 10.1038/ng.3117
- Liu, S., Gao, P., Wang, X., Davis, A. R., Baloch, A. M., and Luan, F. (2014). Mapping of quantitative trait loci for lycopene content and fruit traits in *Citrullus lanatus*. *Euphytica*. 202, 411–426. doi: 10.1007/s10681-014-1308-9
- Liu, S., Gao, Z., Wang, X., Luan, F., Dai, Z., Yang, Z., et al. (2021). Nucleotide variation in the phytoene synthase (CIPs1) gene contributes to golden flesh in watermelon (*Citrullus lanatus* L.). *Theor. Appl. Genet.* 135, 185–200. doi: 10.1007/s00122-021-03958-0
- Liu, L., Shao, Z., Zhang, M., and Wang, Q. (2015). Regulation of carotenoid metabolism in tomato. *Mol. Plant* 8, 28–39. doi: 10.1016/j.molp.2014.11.006
- Lu, H. W., Miao, H., Tian, G. L., Wehner, T. C., Gu, X. F., and Zhang, S. P. (2015). Molecular mapping and candidate gene analysis for yellow fruit flesh in cucumber. *Mol. Breed* 35, 64. doi: 10.1007/s11032-015-0263-z
- Lu, S., Zhang, Y., Zhu, K., Yang, W., Ye, J., Chai, L., et al. (2018). The citrus transcription factor *CsMADS6* modulates carotenoid metabolism by directly regulating carotenogenic genes. *Plant Physiol.* 176, 2657–2676. doi: 10.1104/pp.17.01830
- Mizuno, K., Tokiwano, T., and Yoshizawa, Y. (2017). Gene expression analysis of enzymes of the carotenoid biosynthesis pathway involved in  $\beta$ -cryptoxanthin accumulation in wild raspberry, *Rubus palmatus*. *Biochem. Biophys. Res. Commun.* 484, 845–849. doi: 10.1016/j.bbrc.2017.01.186
- Pei, S., Liu, Z., Wang, X., Luan, F., Dai, Z., Yang, Z., et al. (2021). Quantitative trait loci and candidate genes responsible for pale green flesh colour in watermelon (*Citrullus lanatus*). *Plant Breed.* 140, 349–359. doi: 10.1111/pbr.12908
- Peng, G., Wang, C. Y., Song, S., Fu, X. M., Azam, M., Grierson, D., et al. (2013). The role of 1-deoxy-D-xylulose-5-phosphate synthase and phytoene synthase gene family in citrus carotenoid accumulation. *Plant Physiol.* *Biochem.* 71, 67–76. doi: 10.1016/j.plaphy.2013.06.031
- Pereira-Castro, I., and Moreira, A. (2021). On the function and relevance of alternative 3-UTRs in gene expression regulation. *WIREs RNA*. 12, e1653. doi: 10.1002/wrna.1653
- Pin, L., Na, L., Hui, L., Huihui, G., and Wen-en, Z. (2015). Changes in carotenoid profiles and in the expression pattern of the genes in carotenoid metabolisms during fruit development and ripening in four watermelon cultivars. *Food Chem.* 174, 52–59. doi: 10.1016/j.foodchem.2014.11.022
- Ray, J., Moureau, P., Bird, C., Bird, A., Grierson, D., Maunders, M., et al. (1992). Cloning and characterization of a gene involved in phytoene synthesis from tomato. *Plant Mol. Biol.* 19, 401–404. doi: 10.1007/BF00023387
- Rodriguez-Urbe, L., Guzman, I., Rajapakse, W., Richins, R. D., and Oconnell, M. A. (2012). Carotenoid accumulation in orange-pigmented Capsicum annum fruit, regulated at multiple levels. *J. Exp. Bot.* 63, 517–526. doi: 10.1093/jxb/err302
- Saini, R. K., Nile, S. H., and Park, S. W. (2015). Carotenoids from fruits and vegetables: Chemistry, analysis, occurrence, bioavailability and biological activities. *Food Res. Int.* 76, 735–750. doi: 10.1016/j.foodres.2015.07.047
- Shen, J., Liu, J., Xie, K., Xing, F., Xiong, F., Xiao, J., et al. (2017). Translational repression by a miniature inverted-repeat transposable element in the 3' untranslated region. *Nat. Commun.* 8, 14651. doi: 10.1038/ncomms14651
- Sobrinho-Mengual, G., Alvarez, D., Twyman, R. M., Gerrish, C., Fraser, P. D., Capell, T., et al. (2024). Activation of the native *PHYTOENE SYNTHASE 1* promoter by modifying near-miss cis-acting elements induces carotenoid biosynthesis in embryogenic rice callus. *Plant Cell Rep.* 43, 118. doi: 10.1007/s00299-024-03199-7
- Tzuri, G., Zhou, X., Chayut, N., Yuan, H., Portnoy, V., Meir, A., et al. (2015). A golden SNP in *CmOr* governs the fruit flesh color of melon (*Cucumis melo*). *Plant J.* 82, 267–279. doi: 10.1111/tpj.12814
- Xie, Y. G., Xiao, Y., Yu, M. Y., and Yang, W. C. (2024). Acyl-CoA synthetase 1 plays an important role on pollen development and male fertility in tomato. *Plant Physiol. Biochem.* 208, 108523. doi: 10.1016/j.plaphy.2024.108523
- Xiumin, F., Chao, F., Chunyan, W., Xueren, Y., Pengjun, L., Grierson, D., et al. (2014). Involvement of multiple phytoene synthase genes in tissue- and cultivar-specific accumulation of carotenoids in loquat. *J. Exp. Bot.* 65, 4679–4689. doi: 10.1093/jxb/eru257
- Yang, T., Ali, M., Lin, L., Li, P., He, H., Zhu, Q., et al. (2023). Recoloring tomato fruit by CRISPR/Cas9-mediated multiplex gene editing. *Hortic. Res.* 10, uhac214. doi: 10.1093/hr/uhac214
- Zhang, D., Ai, G., Ji, K., Huang, R., Chen, C., Yang, Z., et al. (2023). *EARLY FLOWERING* is a dominant gain-of-function allele of *FANTASTIC FOUR 1/2c* that promotes early flowering in tomato. *Plant Biotechnol. J.* 22, 698–711. doi: 10.1111/pbi.14217
- Zhang, J., Sun, H., Guo, S., Ren, Y., Li, M., Wang, J., et al. (2020). Decreased protein abundance of lycopene  $\beta$ -cyclase contributes to red flesh in domesticated watermelon. *Plant Physiol.* 183, 1171–1183. doi: 10.1104/pp.19.01409
- Zhou, X., Rao, S., Wrightstone, E., Sun, T., Lui, A. C. W., Welsch, R., et al. (2022). Phytoene synthase: the key rate-limiting enzyme of carotenoid biosynthesis in plants. *Front. Plant Sci.* 13. doi: 10.3389/fpls.2022.884720
- Zhu, G., Wang, S., Huang, Z., Zhang, S., Liao, Q., Zhang, C., et al. (2018). Rewiring of the fruit metabolome in tomato breeding. *Cell.* 172, 249–61.e12. doi: 10.1016/j.cell.2017.12.019